

Ultraviolet Photometry and Reddening Estimation of 105 Galactic Open Clusters

T. Ramezani¹ , E. Paunzen¹ , A. Gorodilov¹  and O. I. Pintado² 

¹ *Department of Theoretical Physics and Astrophysics, Masaryk University,
Kotlářská 2, 611 37 Brno, Czechia
(E-mail: epaunzen@physics.muni.cz)*

² *Consejo Nacional de Investigaciones Científicas y Técnicas, Argentina*

Received: March 23, 2025; Accepted: March 31, 2025

Abstract. This paper focuses on observing unstudied Galactic open clusters in the Ultraviolet (UV) wavelength range and analyzing their photometric data. The Gaia Data Release 3 (DR3) enables us to precisely study known Galactic open clusters. We conducted observations using the 1.54-meter Danish Telescope (DK1.54) in Chile and the 2.15-meter telescope at the Complejo Astronómico El Leoncito (CASLEO) in Argentina, employing UV filters. Furthermore, we have collected available photometric and astrometric data for our observed clusters. We aim to estimate the reddening of Galactic open clusters using UV photometry. We applied isochrone fitting to determine the reddening of the clusters using well-known members. As a final result, we present the reddening values of 105 Galactic open clusters in the UV, as determined by our photometry.

Key words: Open Clusters, Gaia, Ultraviolet, Photometry

1. Introduction

Star clusters, particularly open clusters, serve as essential laboratories for understanding stellar formation, evolution, and dynamics. Since stars within a cluster share a common origin, distance, and age, their study provides crucial insight into the broader processes of stellar evolution (Krause et al., 2020). By analyzing star clusters, we can refine our models of stellar formation and lifecycles, such as those governed by mass, composition, and environment. Studying these clusters in the Ultraviolet (UV) wavelengths is particularly important because UV observations are sensitive to young, hot, and massive stars (Hillier, 2020). These stars emit most of their light in the UV, making this wavelength regime critical for understanding the early stages of stellar evolution and the Interstellar Medium (ISM). One of the key challenges in studying star clusters is interstellar reddening (absorption or extinction; Pandey et al., 2003). This effect is caused by dust grains in the ISM that scatter and absorb starlight, causing the light from stars to shift toward redder wavelengths (Cardelli et al., 1989). The amount of reddening is a function of the dust column density and the object's location within the Galaxy. Correcting for this reddening is essential for accurately determining stellar properties such as temperature and luminosity. Extinction models, such as the Fitzpatrick (1999)

model, are commonly used to correct for these effects. These models help to remove the distortion introduced by the ISM and allow us to recover the intrinsic colours and magnitudes of stars.

Unfortunately, recent UV observations of star clusters are very scarce. Only a few Well-studied ones are also analysed in the UV (Sindhu et al., 2018). The Ultra Violet Imaging Telescope (UVIT) consortium presented some results for well-known star clusters (Jadhav et al., 2021).

In this paper, we present the status of our project to observe Galactic open clusters to study their extinction characteristics using our own observed Johnson U and archival Gaia BP , RP , and G photometry.

2. Target selection and observations

For the first case study of our project, we selected 105 southern star clusters from the list of Hunt & Reffert (2023) which are not too extended on the sky. This catalogue contains the parameters (age, reddening, and distance) and positional information of 7 167 star clusters, including moving groups, with over 700 newly discovered high-confidence clusters. They used the widely applied Hierarchical Density-Based Spatial Clustering of Applications with Noise (HDBSCAN) algorithm (McInnes et al., 2017).

We conducted observations using the 1.54-meter Danish Telescope (DK1.54) in Chile and the 2.15-meter telescope at the Complejo Astronómico El Leoncito (CASLEO) in Argentina, employing UV filters.

The DK1.54 was equipped with the Danish Faint Object Spectrograph and Camera (DFOSC) using a $2k \times 2k$ thinned Loral CCD chip with a field of view (FOV) of 12×12 arc minutes. The 2.15-meter Jorge Sahade reflector at CASLEO was using a $2k \times 2k$ Roper Scientific Versarray 2048B camera with a FOV of about nine arc minutes.

The exposure time for each cluster is 300 seconds, with at least two observations for each cluster.

3. Data Reduction

The basic CCD reductions (bias-subtraction, dark correction, and flat-fielding) were performed with standard IRAF v2.17 routines. We removed cosmic rays whenever needed before calculating the Point Spread Function (PSF) and the instrumental magnitude for all stars.

As the next step, we matched the observed fields using the Atlas of Large-Area Digital Image Navigation (Aladin). For this, we used the IRAF task “xy2sky” to transform pixel coordinates (x , y) into the celestial coordinates (RA, DEC). After a rotation of 270 degrees, we could compare them with external catalogues.

For our purposes, we used the Gaia DR3 (Babusiaux et al., 2023) and its photometry (BP , RP , and G magnitudes) for the matching process. This was done by a newly

developed pipeline software¹ based on the Match Program², which uses the FOCAS algorithm (Valdes et al., 1995). The script takes the Gaia data and our objects in .CSV format as input data. Loading confirmed cluster members representing main sequence stars into the script is also possible. We used Hunt & Reffert (2023) catalogue, which is based on Gaia DR3 data, to define members. We then filtered the matched stars for cluster members.

Instrumental magnitudes are typically uncalibrated values from the instrument, which depend on the specific setup (filters, detectors, and exposure times). The Gaia DR3 provides flux-calibrated low-resolution spectrophotometry (BP/RP spectra) for about 200 million sources in the wavelength range from 330 to 1050 nm (Gaia Collaboration et al., 2023). From these spectra, synthetic photometry can be derived for any passband. Existing observations can be reproduced within a few per cent over a wide range of magnitudes and colour for wide and medium bands, such as Johnson U , and with up to millimag accuracy when synthetic photometry is standardised for external sources. We first checked the available standard U photometry using The General Catalogue of Photometric Data³. No offsets or systematics were detected.

As the last step, we transformed our instrumental magnitudes to standard ones as described by Bessell (2005).

4. Estimating the reddening values

We generated colour-colour diagrams from Colour-Magnitude Diagrams (CMDs), including U photometry and fitted the filtered stars to find their extinction in each colour from the main sequence standard line for the different colour combinations. The standard lines are taken from the Padova database of stellar evolutionary tracks and isochrones (Bressan et al., 2012).

Fitting is done manually, using a GUI interface that allows the standard main sequence to be shifted along two axes corresponding to the combination of colours selected. The script calculates the errors for a confidence interval of 99.73%. A tutorial on the use of pipelines is available in the README.md file.

We get the reddening from U in the independent colour-colour diagram of age, distance, and metallicity. We estimate the reddening for all our observed clusters in different passbands.

Figure 1 shows the Colour–Colour diagrams of different clusters and filter combinations. The green dots are matched non-members, and the pink triangles are members from Hunt & Reffert (2023).

In Table 1, we present the name of the clusters, their coordinates in RA and DEC, different extinction ratios, uncertainties of each extinction’s ratios, mean value of extinctions, the distance and log age from the Hunt & Reffert (2023) catalogue. Only

¹<https://github.com/PoruchikRzhevsky/Match-pipeline>

²<http://spiff.rit.edu/match/>

³<https://gepd.physics.muni.cz/>

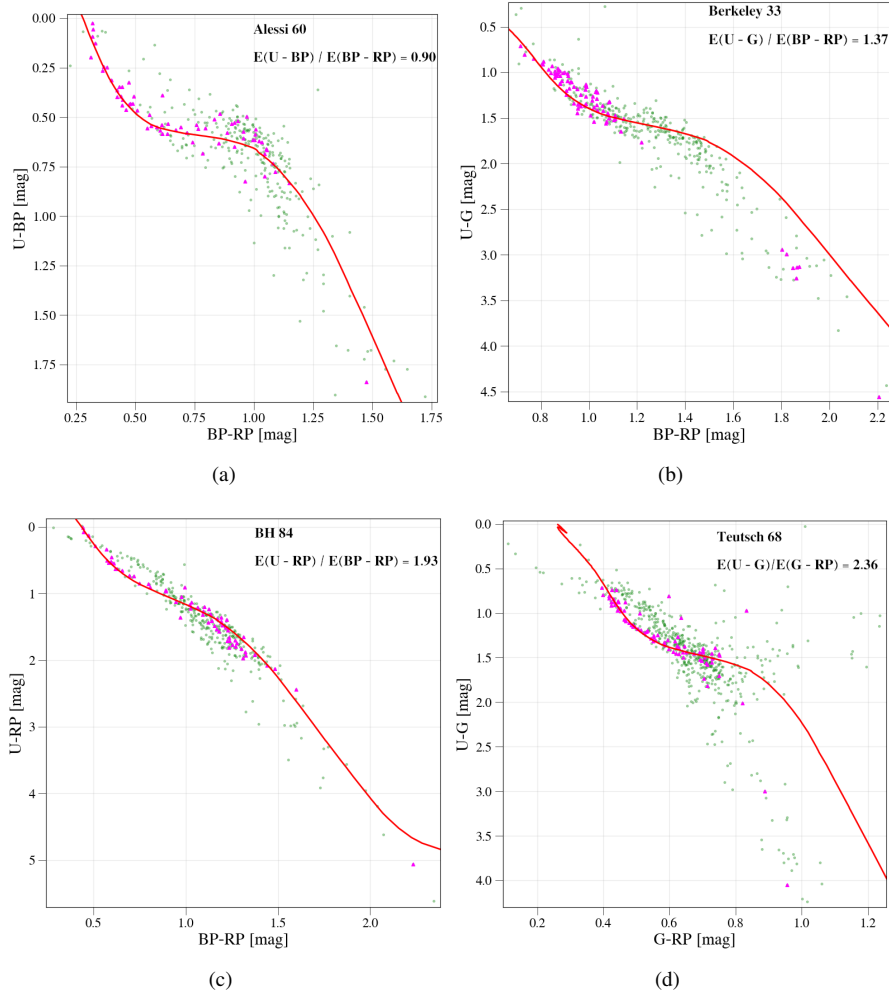


Figure 1. Colour–Colour diagrams of different clusters and filter combinations. The standard lines are taken from Bressan et al. (2012). The green dots are matched non-members and pink triangles are members from Hunt & Reffert (2023).

cluster BH 140 does not have log age in their catalogue. In its complete form, this table is only available at the CDS or upon request.

Table 1. Coordinates, reddening values, and uncertainties of clusters. In its complete form, this table is only available at the CDS or upon request. The first page is printed here for guidance regarding its form and content. The columns denote: (1) Clusters' name. (2) Right ascension (J2000; Gaia DR3). (3) Declination (J2000; GaiaDR3). (4) $E(U - BP)/E(BP - RP)$. (5) $E(U - G)/E(BP - RP)$. (6) $E(U - RP)/E(BP - RP)$. (7) $E(U - G)/E(G - RP)$. (8) $E(U - G)/E(BP - G)$. (9) Uncertainty of $E(U - BP)/E(BP - RP)$. (10) Uncertainty of $E(U - G)/E(BP - RP)$. (11) Uncertainty of $E(U - RP)/E(BP - RP)$. (12) Uncertainty of $E(U - G)/E(G - RP)$. (13) Uncertainty of $E(U - G)/E(BP - G)$. (14) Mean extinction. (15) Distance (kpc). (16) $\log t$.

(1)	(2)	(3)	(4)	(5)	(6)	(7)	(8)	(9)	(10)	(11)	(12)	(13)	(14)	(15)	(16)
Alessi_17	113.853	-15.092	1.08	1.36	2.01	2.08	3.78	0.28	0.11	0.17	0.76	0.41	2.06	3.92	8.38
Alessi_60	105.615	-1.120	0.90	1.29	1.90	2.03	2.09	0.14	0.09	0.08	0.22	0.20	1.64	2.64	8.68
Berkeley_33	104.454	-13.226	0.98	1.37	1.98	2.24	3.45	0.08	0.10	0.08	0.29	0.16	2.00	4.73	8.68
BH_72	142.843	-53.041	1.30	1.68	2.30	2.18	2.98	0.55	0.56	0.57	0.80	0.88	2.09	4.51	8.23
BH_84	150.334	-58.217	0.92	1.33	1.93	2.21	3.22	0.12	0.13	0.13	0.34	0.35	1.92	3.80	8.21
BH_87	151.162	-55.377	1.13	1.54	2.13	2.52	3.71	0.11	0.10	0.08	0.21	0.27	2.21	2.18	8.15
BH_111	167.317	-63.830	0.91	1.30	1.91	2.15	3.32	0.23	0.24	0.22	0.51	0.53	1.92	2.46	8.43
BH_132	186.725	-64.065	0.85	1.32	1.85	1.93	3.45	0.31	0.32	0.32	0.46	0.32	1.88	2.47	7.98
BH_140	193.454	-67.182	1.16	1.55	2.17	2.84	3.44	0.06	0.07	0.07	0.38	0.39	2.23	4.60	
CWNU_95	223.299	-54.108	0.59	1.00	1.63	1.63	2.60	0.18	0.17	0.18	0.68	0.74	1.49	1.05	7.37
CWNU_1733	114.240	-26.321	0.39	0.89	1.45	1.51	2.11	0.27	0.32	0.28	0.71	0.80	1.27	1.73	8.30
Czemik_29	112.095	-15.399	1.08	1.41	2.08	2.44	3.66	0.09	0.10	0.07	0.32	0.21	2.13	3.51	8.39

5. Analysis

Let us recall that stars in galaxies are born in molecular clouds (MCs). The gravitational collapse of the dense regions in the ISM of galaxies is an important mechanism to form star clusters (Keilmann *et al.*, 2024). Dust is made up of heavy elements resulting from star nuclear burning. Dust grains are formed by reprocessing these heavy elements in the interstellar medium after they are expelled from stars by winds and explosions (Draine, 2003).

Dust (and gas) significantly affects light propagation, scattering, and absorbing photons from UV to infrared wavelengths, leading to extinction and reddening effects in astronomical observations (Schlafly & Finkbeiner, 2011). There are two different effects of extinction: 1) From the molecular cloud that the star cluster is born from; 2) From the ISM between the observer and star cluster.

Dust is not symmetrically distributed throughout space because of supernova explosions, stellar winds, magnetic fields, and star formation variations. Another complication is the composition of the ISM, which directly affects the reddening law, i.e. the variation of extinction with wavelength. Therefore, the reddening law and the amount of extinction depend on the line of sight. It is well known that the Galactic disk has regions with an extinction as high as five magnitudes per kpc (Neckel & Klare, 1980).

Expressing the extinction law is not unique in the literature; it has been common practice to use the ratios of two colours, for example, $E(U - B)/E(B - V)$. Using $A(V)$

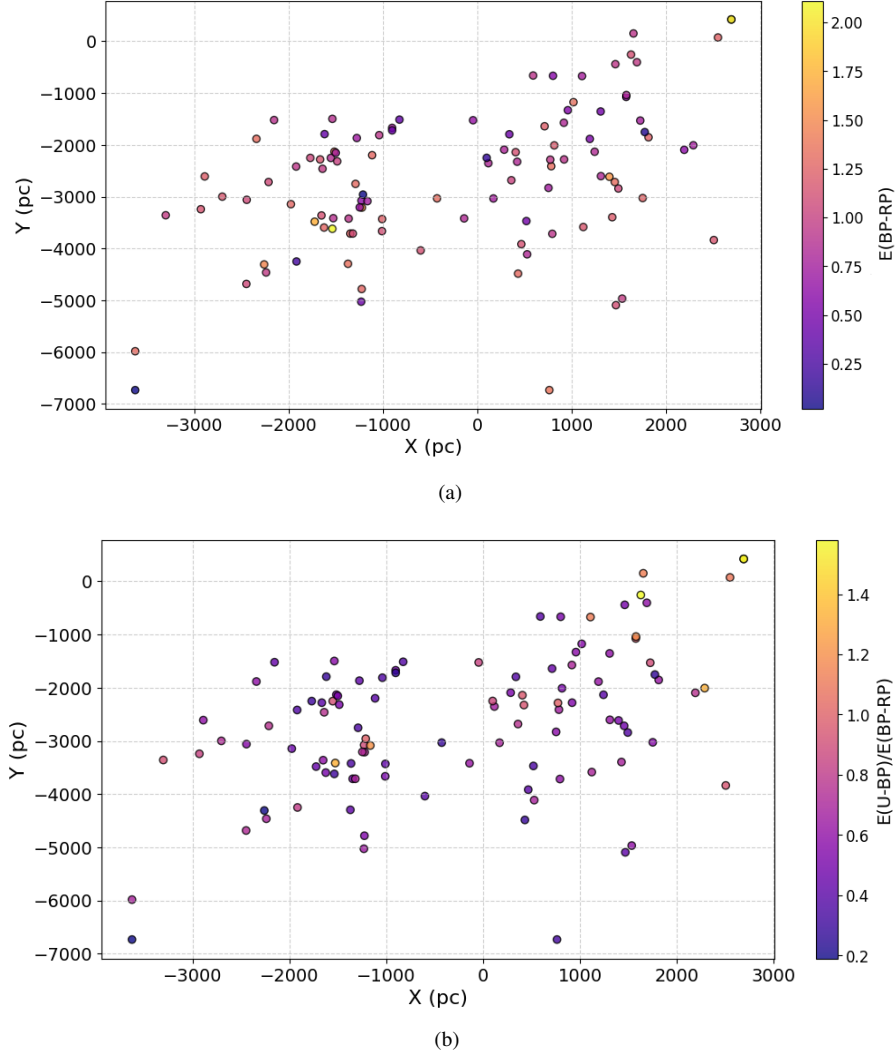


Figure 2. The upper panel shows the extinction in $(BP-RP)$. The lower panel shows the reddening ratio $E(U-BP)/E(BP-RP)$ for the 105 observed clusters in the $[X, Y]$ coordinate system around the Sun at $[0, 0]$, respectively.

as the reference extinction in the visual is arbitrary (Cardelli et al., 1989).

In Fig. 2, we present the results of our extinction estimation in $[X, Y]$ coordinates. The X coordinate is in the direction of the Galactic centre, whereas Y is in the direction of the disk rotation. The Sun is located at $[0, 0]$, respectively. Because all studied star clusters are located in the Galactic disk, we do not consider the third coordinate $[Z]$ for

our analysis.

With very few exceptions, the extinction is increasing for more distant clusters (Fig. 2, upper panel). This is what the current models predict, and it lends confidence in our fitting procedure.

The distribution of the reddening ratio (Fig. 2, lower panel) shows exciting features. For example, there is a continuous transition in the direction $[-3000, -3000]$, some sudden changes on small scales $[-1000, -3000]$, and no changes in certain lines of sight. It proves the capability to trace the ISM with extinction estimates of star clusters.

6. Conclusions and Outlook

It is well known that photometric observations in the UV region help to describe the extinction law and the total absorption. Unfortunately, because of the inefficiency of modern CCD detectors, such observations are not very common any more. On the other hand, the number of star clusters is constantly increasing, caused by the excellent astrometric data of the Gaia satellite mission.

Here, we present our first case study using the synergy of ground-based UV observations and Gaia *BP*, *RP*, and *G* photometry to analyse star clusters. High-precision PSF photometry using published membership probabilities and a matching routine resulted in a unique data set of mainly unstudied open clusters.

Fitting standard main sequences, which are independent of age, metallicity and distance, allowed us to get absorption values and reddening laws toward 105 open clusters. Detailed maps show that our current models could be proven and have the potential to study the characteristics of the ISM in more detail.

As the next step, we plan to observe more Galactic open clusters and generate a reddening law map of the visible regions around the Sun. Another approach we will follow is the synthetic Gaia flux-calibrated low-resolution spectrophotometry (BP/RP spectra), which allows for a synthesis of photometry.

Acknowledgements. This work was supported by the grants GAČR 23-07605S, MUNI/A/1077/2022, and MUNI/A/1419/2023. We want to thank doc. RNDr. M. Zejda, Ph.D., RNDr. J. Janík, Ph.D. from the Department of Theoretical Physics and Astrophysics, Masaryk University, Brno, Czechia, and Waldemar Ogloza from Pedagogical University of Cracow, Poland, for helping us with observations.

References

- Babusiaux, C., Fabricius, C., Khanna, S., et al., Gaia Data Release 3. Catalogue validation. 2023, *Astronomy and Astrophysics*, **674**, A32, DOI:10.1051/0004-6361/202243790
- Bessell, M. S., Standard Photometric Systems. 2005, *Annual Review of Astron and Astrophys*, **43**, 293, DOI:10.1146/annurev.astro.41.082801.100251

- Bressan, A., Marigo, P., Girardi, L., et al., PARSEC: stellar tracks and isochrones with the PAdova and TRieste Stellar Evolution Code. 2012, *Monthly Notices of the Royal Astronomical Society*, **427**, 127, DOI:10.1111/j.1365-2966.2012.21948.x
- Cardelli, J. A., Clayton, G. C., & Mathis, J. S., The Relationship between Infrared, Optical, and Ultraviolet Extinction. 1989, *Astrophysical Journal*, **345**, 245, DOI:10.1086/167900
- Draine, B. T., Interstellar Dust Grains. 2003, *Annual Review of Astron and Astrophys*, **41**, 241, DOI:10.1146/annurev.astro.41.011802.094840
- Fitzpatrick, E. L., Correcting for the Effects of Interstellar Extinction. 1999, *Publications of the ASP*, **111**, 63, DOI:10.1086/316293
- Gaia Collaboration, Montegriffo, P., Bellazzini, M., et al., Gaia Data Release 3. The Galaxy in your preferred colours: Synthetic photometry from Gaia low-resolution spectra. 2023, *Astronomy and Astrophysics*, **674**, A33, DOI:10.1051/0004-6361/202243709
- Hillier, D. J., UV Spectroscopy of Massive Stars. 2020, *Galaxies*, **8**, DOI:10.3390/galaxies8030060
- Hunt, E. L. & Reffert, S., Improving the open cluster census. II. An all-sky cluster catalogue with Gaia DR3. 2023, *Astronomy and Astrophysics*, **673**, A114, DOI:10.1051/0004-6361/202346285
- Jadhav, V. V., Pennock, C. M., Subramaniam, A., Sagar, R., & Nayak, P. K., UOCS - III. UVIT catalogue of open clusters with machine learning-based membership using Gaia EDR3 astrometry. 2021, *Monthly Notices of the RAS*, **503**, 236, DOI:10.1093/mnras/stab213
- Keilmann, E., Kabanovic, S., Schneider, N., et al., Molecular cloud matching in CO and dust in M33: II. Physical properties of giant molecular clouds. 2024, *Astronomy and Astrophysics*, **692**, A226, DOI:10.1051/0004-6361/202451451
- Krause, M. G. H., Offner, S. S. R., Charbonnel, C., et al., The Physics of Star Cluster Formation and Evolution. 2020, *Space Science Reviews*, **216**, 64, DOI:10.1007/s11214-020-00689-4
- McInnes, L., Healy, J., & Astels, S., hdbscan: Hierarchical density based clustering. 2017, *The Journal of Open Source Software*, **2**, DOI:10.21105/joss.00205
- Neckel, T. & Klare, G., The spatial distribution of the interstellar extinction. 1980, *Astronomy and Astrophysics, Supplement*, **42**, 251
- Pandey, A. K., Upadhyay, K., Nakada, Y., & Ogura, K., Interstellar extinction in the open clusters towards galactic longitude around 130^{deg} . 2003, *Astronomy and Astrophysics*, **397**, 191, DOI:10.1051/0004-6361:20021509
- Schlafly, E. F. & Finkbeiner, D. P., Measuring Reddening with Sloan Digital Sky Survey Stellar Spectra and Recalibrating SFD. 2011, *Astrophysical Journal*, **737**, 103, DOI:10.1088/0004-637X/737/2/103

- Sindhu, N., Subramaniam, A., & Radha, C. A., Ultraviolet stellar population of the old open cluster M67 (NGC 2682). 2018, *Monthly Notices of the RAS*, **481**, 226, DOI:[10.1093/mnras/sty2283](https://doi.org/10.1093/mnras/sty2283)
- Valdes, F. G., Campusano, L. E., Velasquez, J. D., & Stetson, P. B., FOCAS Automatic Catalog Matching Algorithms. 1995, *Publications of the ASP*, **107**, 1119, DOI:[10.1086/133667](https://doi.org/10.1086/133667)